Supporting Information

Stable electrical-conductive, highly flame-retardant foam composites generated from reduced graphene oxide and silicone resin coatings

Qian Wu [a, 1], Chun Liu [a, 1], Longcheng Tang [a], Yue Yan [a], Huayu Qiu [a,c], Yongbing Pei [a,c] *, Michael J. Sailor [a,b], and Lianbin Wu [a,c] *

a Key Laboratory of Organosilicon Chemistry and Materials Technology of Ministry of Education, Hangzhou Normal University, Hangzhou, 311121, P. R. China

b Department of Chemistry and Biochemistry, University of California, San Diego, La Jolla, California 92093, United States

c Collaborative Innovation Center of Zhejiang Province for Manufacturing of Fluorine Silicon Fine Chemicals and Materials, Hangzhou Normal University, Hangzhou, 311121, P. R. China

Corresponding authors: wulianbin@hznu.edu.cn, peiyongbing@hznu.edu.cn

1 These authors contributed equally to this work.

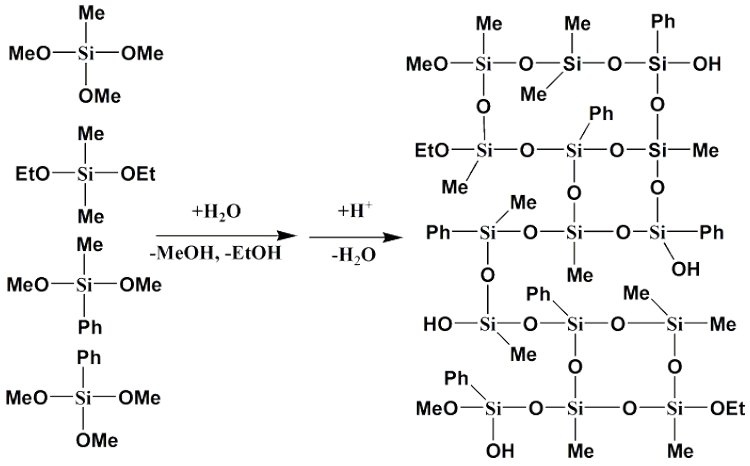

Fig. S1. The synthesis scheme of silicone resin used in this study. The silicone consists of a mixture of dimethyl siloxane, methy phenyl siloxane and monophenyl siloxane components.

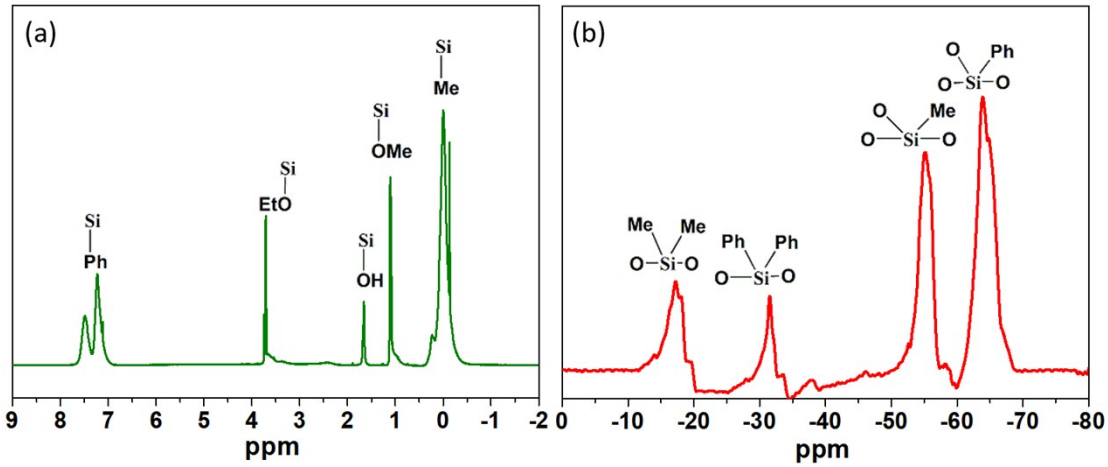

Fig. S2. ^{1}H (a) and ^{29}Si (b) nuclear magnetic resonance (NMR) spectra of the as-synthesized silicone resin. Relevant functional groups are assigned.

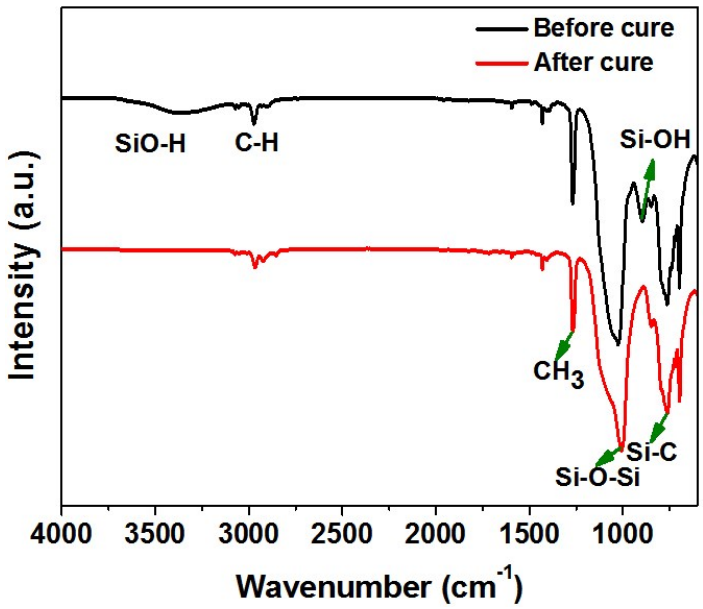

Fig. S3. Fourier transformed infrared (FTIR) spectra of the silicone resin before and after curing. The broad band appearing at 3400 cm^{-1} is assigned to Si-OH species, bands at 2880 and 2970 cm^{-1} are assigned to C-H stretching vibrations, The band at 1220 cm^{-1} is assigned to the CH_3 symmetric deformation, the band at 1010 cm^{-1} is assigned to the Si-O-Si stretch and the band at 760 cm^{-1} is assigned to the Si-C stretch.

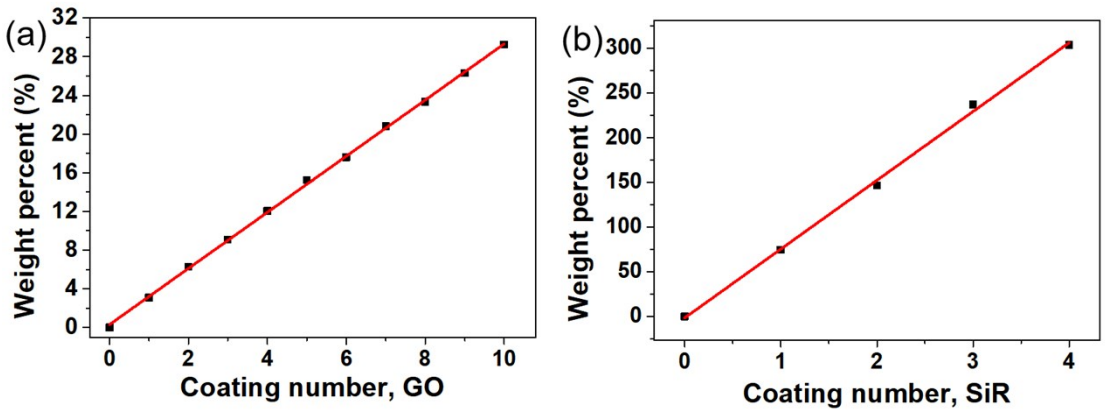

Fig. S4. Percentage of mass gained by the PU samples upon repeated dip-coating in (a) graphene oxide (GO) and (b) silicone resin (SiR) solutions, as described in the text. For the samples in (a), the successive GO coatings were applied to a pristine polyurethane sample. For the samples in (b), the successive coatings were applied to PU sample that had been coated with GO and then reduced to RGO, as described in the text.

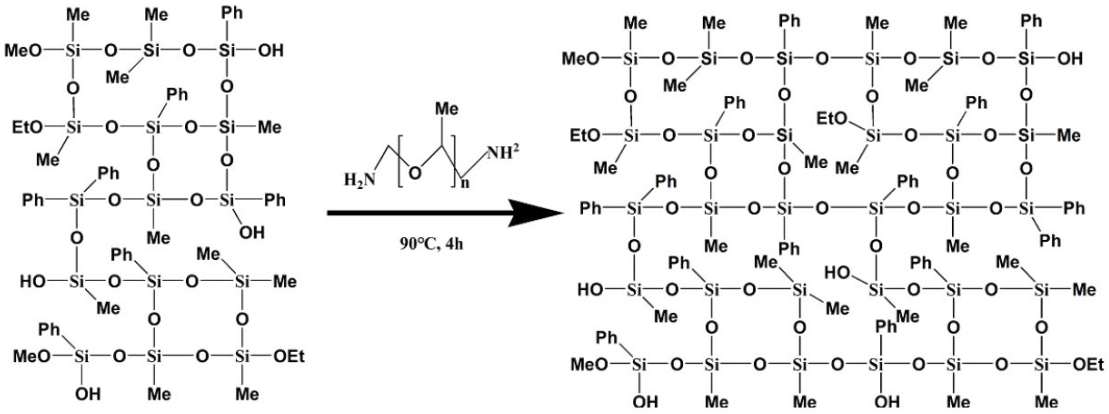

Fig. S5. Schematic depicting the proposed mechanism of crosslinking for the SiR composite coating.

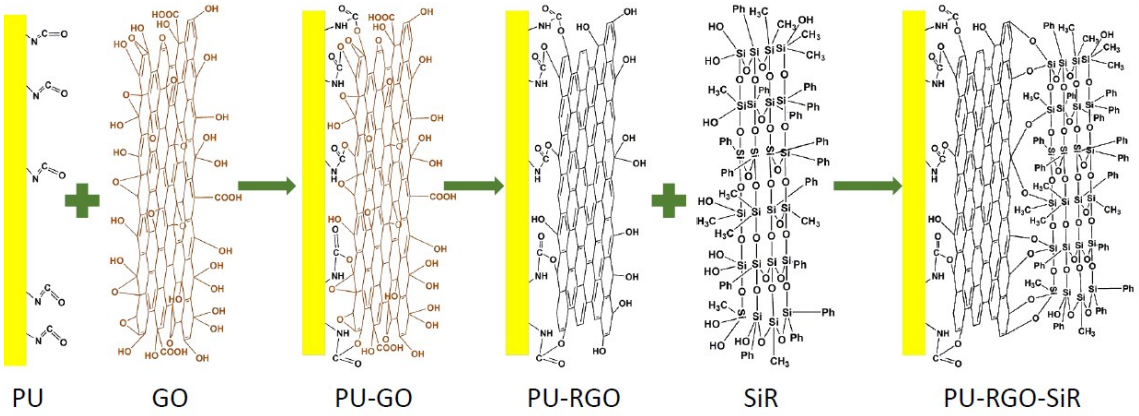

Fig. S6. Schematic depiction of fabrication of the reduced graphene oxide (RGO) coating on the surface of PU foam , and the subsequent deposition of the silicone resin (SiR) coating onto the RGO surface.

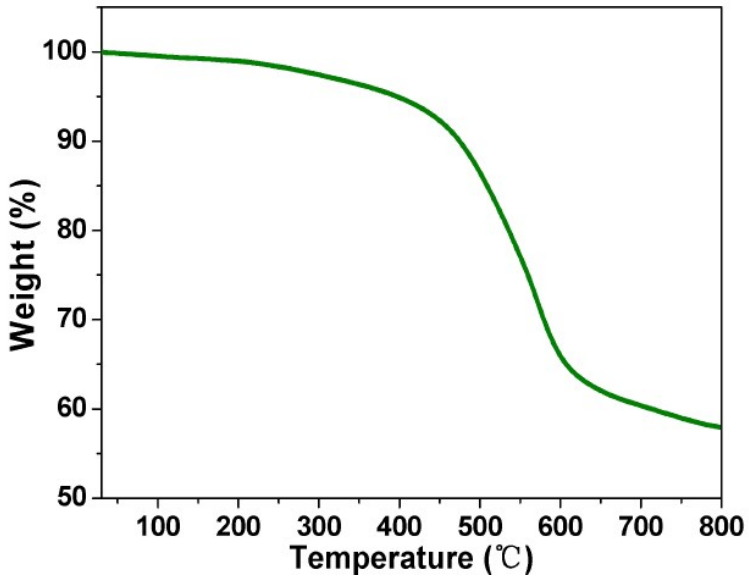

Fig. S7. Thermogravimetric analysis (TGA) of the pure silicone resin (SiR) used as a coating in these studies.

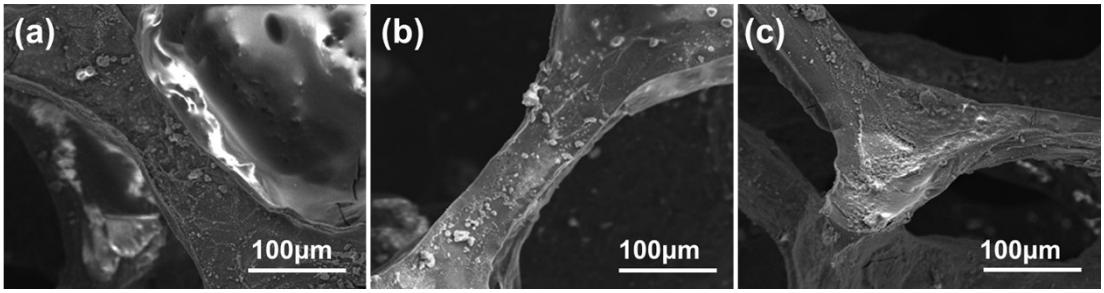

Fig. S8. SEM images of (a) pristine PU-RGO-SiR before and after (b) immersion in hexane solvent for 24 h, and (c) 150 compression tests.

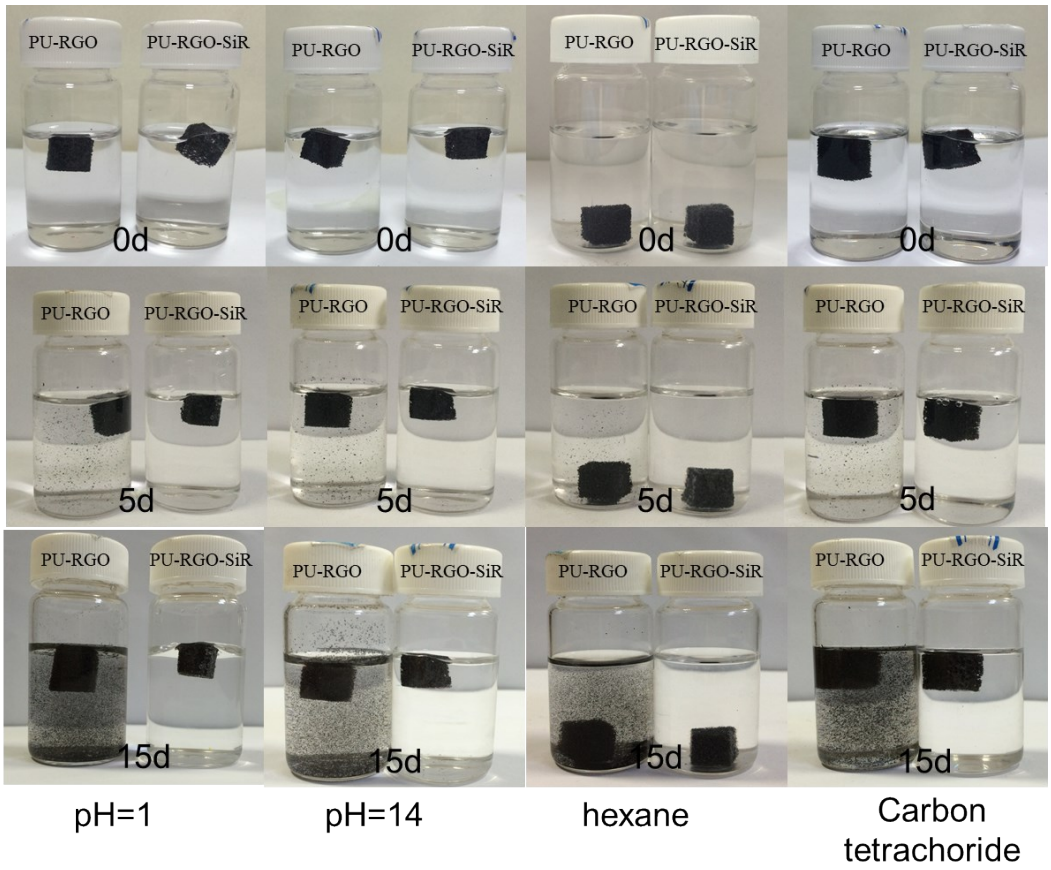

Fig. S9. Photographs of PU-RGO and PU-RGO-SiR samples soaked in aqueous solution at pH 1 and pH 14 and in organic solvents, as indicated, over time: (a) samples immediately after introduction to the pH = 1 aqueous solution ("0d"), and after 5 days ("5d") and 15 days ("15d") of exposure to the liquid; (b) samples immediately after introduction to the pH = 14 aqueous solution ("0d"), and after 5 days ("5d") and 15 days ("15d") of exposure to the liquid; (c) samples immediately after introduction to hexane ("0d"), and after 5 days ("5d") and 15 days ("15d") of exposure to the liquid (d) carbon tetrachloride ("0d"), and after 5 days ("5d") and 15 days ("15d") of exposure to the liquid.

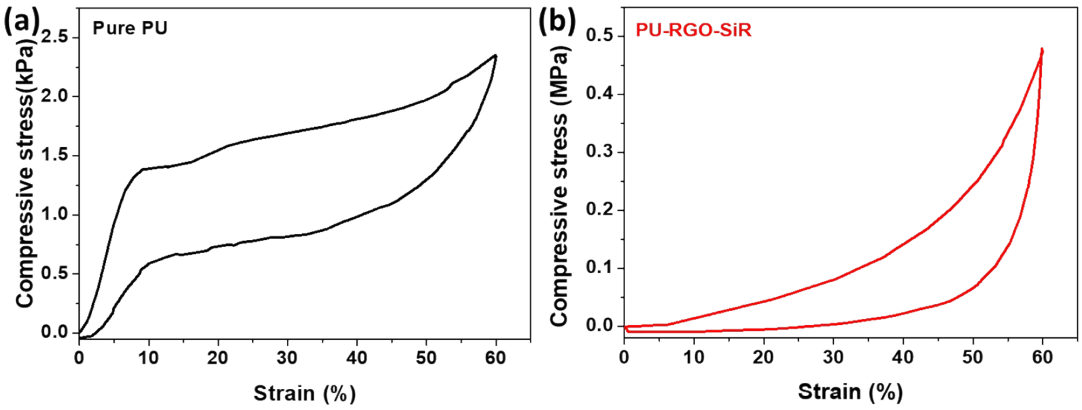

Fig. S10. Compressive stress-strain curves of (a) pure PU and (b) PU-RGO-SiR composites.

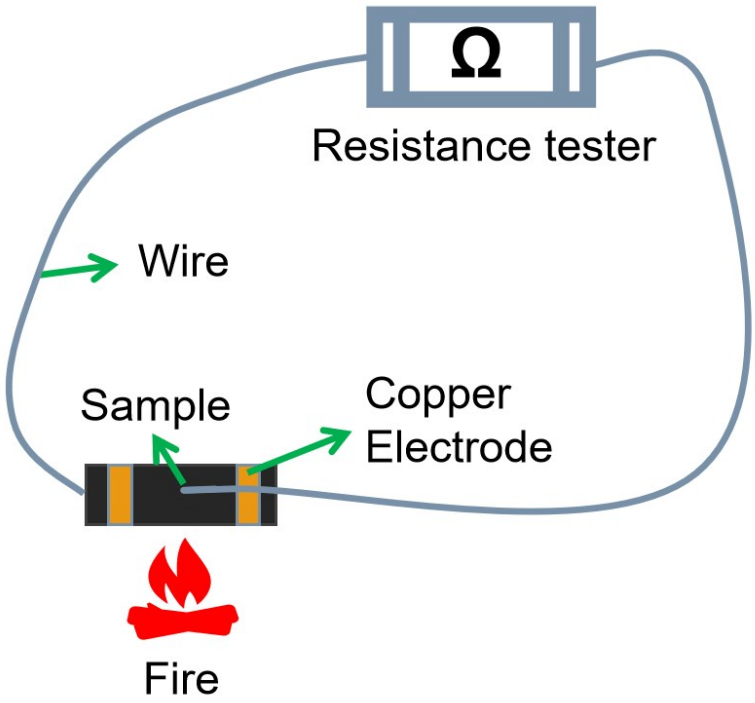

Fig. S11. Schematic diagram of apparatus used to measure sample conductivity changes during exposure to flame.

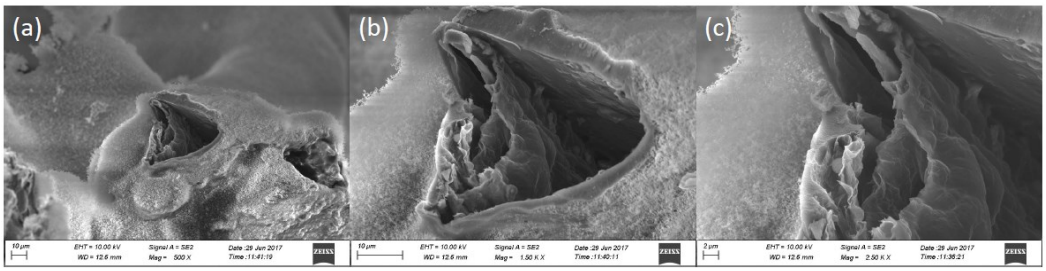

Fig. S12. SEM images of PU-RGO-SiR after complete combustion, this clearly presented RGO layer and the different sides RGO layer are stacked closely together.

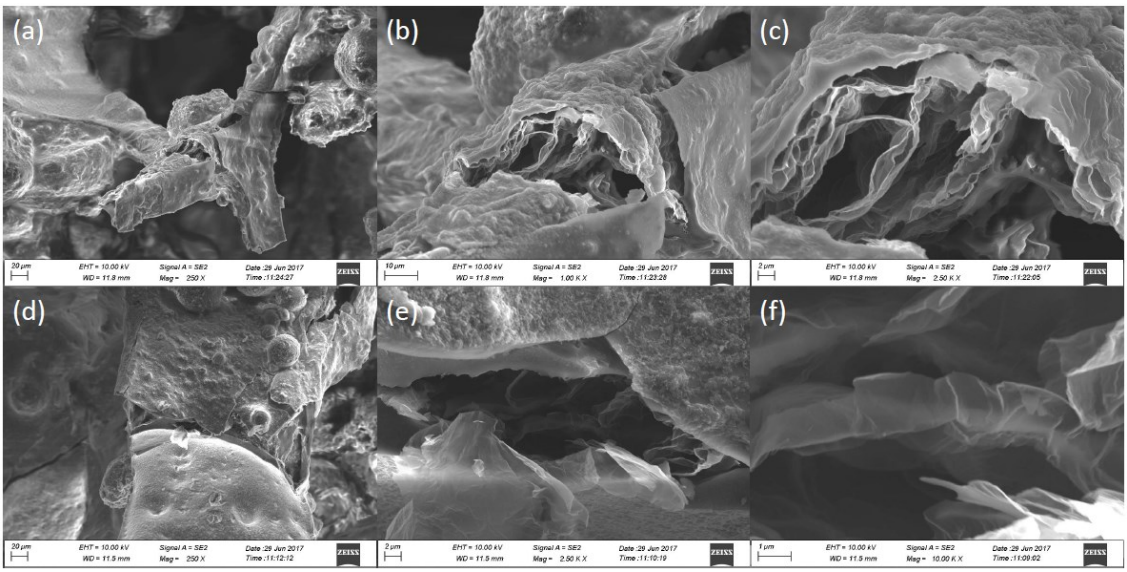

Fig. S13. SEM images of PU-RGO-SiR after complete combustion, (a-e) showing the upper silica crust layer and (f) showing that the RGO inside the silica crust layer is not oxidized after complete combustion.

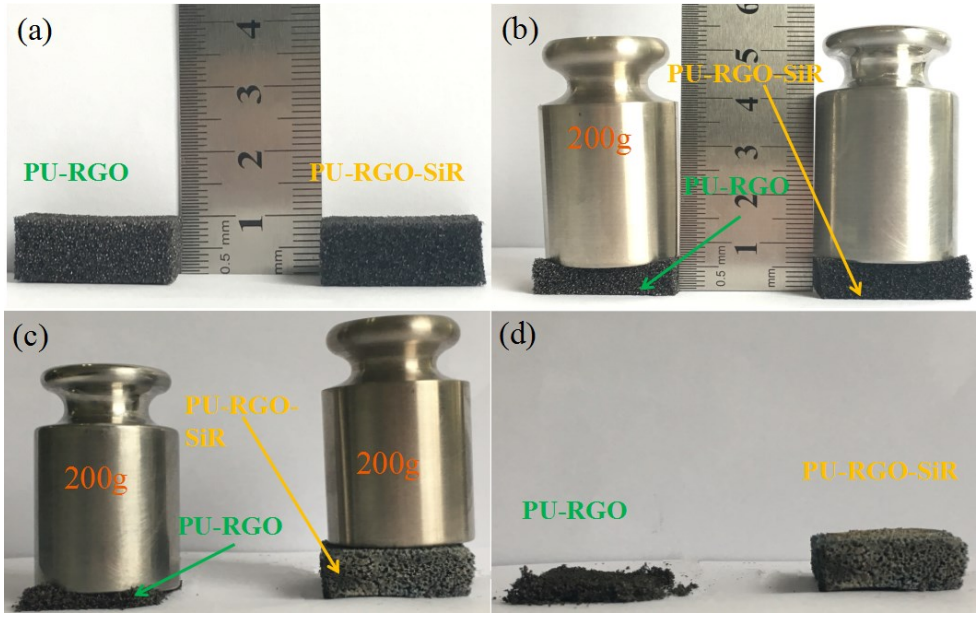

Fig. S14. Compressive strain experiments on PU-RGO and PU-RGO-SiR. Photographs of PU-RGO and PU-RGO-SiR samples show the thickness of PU-RGO and PU-RGO-SiR before loading (a); with a 200g mass loading on top of each sample (b); after a few minutes under the 200 g compressive loading (c); and the foams after being subjected to combustion conditions and stress loading (d). The PU-RGO sample readily collapsed under these conditions, while the PU-RGO-SiR sample retained its shape after complete combustion and stress loading

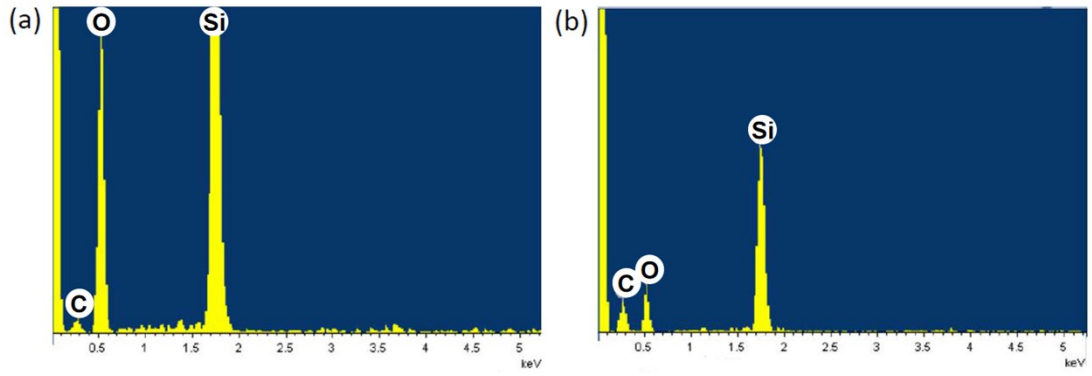

Fig. S15. The SEM-EDX spectra of the PU-RGO-SiR sample after combustion, (a) the white crust and (b) the inner matter.

Video S1

Measurement of change in conductivity of the PU-RGO-SiR sample during combustion, with the sample directly exposed to a flame source for ~100 s. Sample conductivity increased during burning, and the structural integrity and conductivity of the sample were retained.

Video S2

Vertical burning tests of pure PU foam. The pure foam was easily and quickly ignited after direct exposure to a flame source for 1 s, and the sample was completely combusted within 8 s. Sample displayed persistent dripping and smoke during combustion. The specimen dimensions were 125.0±5.0 mm long, 13.0±0.5 mm wide and 10.0±0.5 mm thick.

Video S3

Vertical burning tests of PU-RGO foam. The PU-RGO foam was easily and quickly ignited after direct exposure to a flame source for 3 s, and the sample was completely combusted within 15 s. Unlike the pure PU foam, the sample displayed no dripping of liquid byproducts during combustion. The specimen dimensions were 125.0±5.0 mm long, 13.0±0.5 mm wide and 10.0±0.5 mm thick.

Video S4

Vertical burning tests of PU-SiR foam. The PU-RGO foam was easily and quickly ignited after direct exposure to a flame source for 10 s, and the sample was

completely combusted within 52 s. Unlike the pure PU foam, the sample displayed no dripping of liquid byproducts during combustion. The specimen dimensions were 125.0±5.0 mm long, 13.0±0.5 mm wide and 10.0±0.5 mm thick.

Video S5

Vertical burning tests of PU-RGO-SiR foam. The PU-RGO-SiR foam was easily and quickly ignited after direct exposure to a flame source for 10 s. The sample burned slowly, the flames gradually diminished, and the sample self-extinguished after 14 s. Unlike the pure PU foam, the sample displayed no dripping of liquid byproducts during combustion. The specimen dimensions were 125.0±5.0 mm long, 13.0±0.5 mm wide and 10.0±0.5 mm thick.

Table S1. The comparison of the cone calorimeter data with the reported literature

Sample	pHRR reduction [%]	TSR reduction [%]	Char increment [%]	Ref.
MOFs@PU	50.6	35.5	/	[1]
MoS_2-DOPO	41.3	25.5	12.4	[2]
ZIF-RPUF	21.3	24.0	/	[3]
MXene/chitosan	57.2	71.0	35.7	[4]
Mica-Based Multilayer	54.2	76.5	/	[5]
Si-N-Zn Ternary-hybrids	33.8	63.5	/	[6]
Expandable Graphite	52.7	79.8	38.4	[7]
fGO-PU	32.9	26.1	17.3	[8]
RGO-SiR	65.1	30.3	60.0	This work

[1] S. Zhao, L. Yin, Q. Zhou, C. Liu, K. Zhou, In situ self-assembly of zeolitic imidazolate frameworks on the surface of flexible polyurethane foam: Towards for highly efficient oil spill cleanup and fire safety, Appl. Surf. Sci., 506 (2020) 144700.

[2] M. Zhi, Q. Liu, Y. Zhao, S. Gao, Z. Zhang, Y. He, Novel MoS2–DOPO Hybrid for Effective Enhancements on Flame Retardancy and Smoke Suppression of Flexible Polyurethane Foams, ACS Omega, 5 (2020) 2734-2746.

[3] J. Cheng, D. Ma, S. Li, W. Qu, D. Wang, Preparation of Zeolitic Imidazolate Frameworks and Their Application as Flame Retardant and Smoke Suppression Agent for Rigid Polyurethane Foams, Polymers, 12 (2020).

[4] B. Lin, A.C.Y. Yuen, A. Li, Y. Zhang, T.B.Y. Chen, B. Yu, E.W.M. Lee, S. Peng, W. Yang, H.-D. Lu, Q.N. Chan, G.H. Yeoh, C.H. Wang, MXene/chitosan nanocoating for flexible polyurethane foam towards remarkable fire hazards reductions, J. Hazar. Mater., 381 (2020) 120952.

[5] A. Fahami, J. Lee, S. Lazar, J.C. Grunlan, Mica-Based Multilayer Nanocoating as a Highly Effective Flame Retardant and Smoke Suppressant, ACS Appl. Mater. Inter., (2020).

[6] W. Xu, G. Wang, J. Xu, Y. Liu, R. Chen, H. Yan, Modification of diatomite with melamine coated zeolitic imidazolate framework-8 as an effective flame retardant to enhance flame retardancy and smoke suppression of rigid polyurethane foam, J. Hazar. Mater., 379 (2019) 120819.

[7] P. Acuña, M. Santiago-Calvo, F. Villafañe, M.A. Rodríguez-Perez, J. Rosas, D.-Y. Wang, Impact of expandable graphite on flame retardancy and mechanical properties of rigid polyurethane foam, Polym. Comp., 40 (2019) E1705-E1715.

[8] M. Gao, J. Li, X. Zhou, A flame retardant rigid polyurethane foam system including functionalized graphene oxide, Polym. Comp., 40 (2019) E1274-E1282.